AFWL-TR-
86-132

(2)

EXPERIMENTAL CONFIRMATION OF SUPERPOSITION FROM SMALL-SCALE EXPLOSIONS

B. W. Stump
R. E. Reinke

November 1987

Final Report

Approved for public release: distribution unlimited.

AIR FORCE WEAPONS LABORATORY
Air Force Systems Command
Kirtland Air Force Base, NM 87117-6008

This final report was prepared by the Air Force Weapons Laboratory, Kirtland Air Force Base, New Mexico, Job Order 88091392. Dr. Robert E. Reinke (NTESG) was the Laboratory Project Officer-in-Charge.

When Government drawings, specifications, or other data are used for any purpose other than in connection with a definitely Government-related procurement, the United States Government incurs no responsibility or any obligation whatsoever. The fact that the Government may have formulated or in any way supplied the said drawings, specifications, or other data, is not to be regarded by implication, or otherwise in any manner construed, as licensing the holder, or any other person or corporation; or as conveying any rights or permission to manufacture, use, or sell any patented invention that may in any way be related thereto.

This report has been authored by employees of the United States Government. Accordingly, the United States Government retains a nonexclusive, royalty-free license to publish or reproduce the material contained herein, or allow others to do so, for the United States Government purposes.

This report has been reviewed by the Public Affairs Office and is releasable to the National Technical Information Service (NTIS). At NTIS, it will be available to the general public, including foreign nations.

If your address has changed, if you wish to be removed from our mailing list, or if your organization no longer employs the addressee, please notify AFWL/NTESG, Kirtland Air Force Base, NM 87117-6008 to help us maintain a current mailing list.

This report has been reviewed and is approved for publication.

Robert E Reinke

ROBERT E. REINKE, PhD
Project Officer

FOR THE COMMANDER

Thomas E Bretz

THOMAS E. BRETZ, JR.
Lt Col, USAF
Chief, Applications Br

Carl L Davidson

CARL L. DAVIDSON
Col, USAF
Chief, Civil Engineering Research Div

DO NOT RETURN COPIES OF THIS REPORT UNLESS CONTRACTUAL OBLIGATIONS OR NOTICE ON A SPECIFIC DOCUMENT REQUIRES THAT IT BE RETURNED.

UNCLASSIFIED
SECURITY CLASSIFICATION OF THIS PAGE

REPORT DOCUMENTATION PAGE

1a. REPORT SECURITY CLASSIFICATION Unclassified	1b. RESTRICTIVE MARKINGS AD-A190 663
2a. SECURITY CLASSIFICATION AUTHORITY	3. DISTRIBUTION / AVAILABILITY OF REPORT Approved for public release; distribution unlimited.
2b. DECLASSIFICATION / DOWNGRADING SCHEDULE	
4. PERFORMING ORGANIZATION REPORT NUMBER(S) AFWL-TR-86-132	5. MONITORING ORGANIZATION REPORT NUMBER(S)
6a. NAME OF PERFORMING ORGANIZATION Air Force Weapons Laboratory 6b. OFFICE SYMBOL (If applicable) NTESG	7a. NAME OF MONITORING ORGANIZATION
6c. ADDRESS (City, State, and ZIP Code) Kirtland Air Force Base, NM 87117-6008	7b. ADDRESS (City, State, and ZIP Code)
8a. NAME OF FUNDING / SPONSORING ORGANIZATION 8b. OFFICE SYMBOL (If applicable)	9. PROCUREMENT INSTRUMENT IDENTIFICATION NUMBER
8c. ADDRESS (City, State, and ZIP Code)	10. SOURCE OF FUNDING NUMBERS PROGRAM ELEMENT NO. 62601F; PROJECT NO. 8809; TASK NO. 13; WORK UNIT ACCESSION NO. 92

11. TITLE (Include Security Classification)
EXPERIMENTAL CONFIRMATION OF SUPERPOSITION FROM SMALL-SCALE EXPLOSIONS

12. PERSONAL AUTHOR(S)
Stump, B.W., and Reinke, R.E.

13a. TYPE OF REPORT	13b. TIME COVERED	14. DATE OF REPORT (Year, Month, Day)	15. PAGE COUNT
Final	FROM Jun 84 TO Dec 85	1987 November	40

16. SUPPLEMENTARY NOTATION

17. COSATI CODES			18. SUBJECT TERMS (Continue on reverse if necessary and identify by block number)
FIELD	GROUP	SUB-GROUP	
08	11		Ground motion, High explosive, Ground motion simulation, Explosive arrays, Spectral analysis, Stochastic characterization, Spectral analysis, Geologic inhomogeneity, Linear (over)
19	01		

19. ABSTRACT (Continue on reverse if necessary and identify by block number)

An in situ experimental program is implemented and analyzed to test linear superposition. After separating stochastic and deterministic propagation path effects, direct superposition is experimentally validated for two 5-lb charges spaced as close as 2 m in alluvium. Finite spatial source effects are observed and modeled in the plane passing through two charges separated by 2 to 10 m. The deterministic single-burst waveforms are used to model the multiple burst data. The effects observed and modeled include direct superposition below the corner frequency, shift to lower corner frequency with charge separation, and spectral scalloping. For charges closely spaced (up to 4 m, observed at 20 m, 24 m) the primary effect on the waveform is replicated by a constant delay time between two identical waveforms. For charges spaced by 10 m (observed at 20 m, 30 m) the effects of propagation path differences must be included. These effects result in smoother spectra.

20. DISTRIBUTION / AVAILABILITY OF ABSTRACT ☒ UNCLASSIFIED/UNLIMITED ☐ SAME AS RPT. ☐ OTIC USERS	21. ABSTRACT SECURITY CLASSIFICATION Unclassified
22a. NAME OF RESPONSIBLE INDIVIDUAL Dr. Robert E. Reinke	22b. TELEPHONE (Include Area Code) (505) 844-0484 22c. OFFICE SYMBOL AFWL/NTESG

DD FORM 1473, 84 MAR 83 APR edition may be used until exhausted.
All other editions are obsolete.

SECURITY CLASSIFICATION OF THIS PAGE
UNCLASSIFIED

18. SUBJECT TERMS (continued)

superposition.

CONTENTS

FIGURES

INTRODUCTION

The effect of finite sources on radiated wave fields has received considerable attention from the earthquake source community. Such work has increased our understanding of source phenomenology while improving our ability to estimate ground motions from broad classes of earthquake sources. Finite explosive arrays effects have received far less attention within the seismological literature.

The primary focus of this study is the investigation of finite spatial source effects from chemical explosions. In particular, the interaction of deterministic and stochastic wave propagation with the source characterization problem will be discussed. Evidence supporting linear superposition will be shown. The assumption of linear superposition leads to a predictive capability.

Spatial arrays of chemical explosions are used in a number of different fields. The mining industry uses arrays of explosives in both open pit and subsurface excavation. The spatial distribution of charges and timing of their detonation are used to control the extent of material excavated, the size of the rubble, and the far-field ground motion levels (Refs. 1, 2, and 3). The majority of work in this area has dealt with laboratory and field data resulting in the development of practical relationships for explosive array design (Refs. 4, 5, and 6). Little theoretical work or numerical modeling of these effects has been completed. This type of investigation has not been necessary since the properly scaled experiments in the materials of interest can be conducted.

The second area where arrays of explosives are employed is in the simulation of ground motions from earthquakes (Refs. 7 and 8). Although data from natural events are available, the recurrence interval of great earthquakes has retarded the development of adequate natural data sets. Where site specific data are required and the historical data base is absent, explosive simulation of earthquake environments may help refine loads on engineering structures.

Since the onset of the aboveground test ban treaty, the utilization of high explosive arrays in simulating ground motion environments from nuclear explosions has been the only way to exercise engineering structures (Ref. 9). These studies have primarily focused upon regions where the stress-strain relations are apparently nonlinear. The spatial and temporal dimensions of the source are adjusted to produce motion environments with prescribed amplitudes and pulse widths.

In each of the three previous applications of explosive arrays, the focus has been upon the near source wave field. The radiated energy from these explosive arrays in the far field is of interest to the community responsible for discriminating earthquakes from explosions. In the advent of a comprehensive test ban treaty, one would have to be able to discriminate between a large mining blast (which might be as large as several hundred thousand pounds of explosives) and a low-yield nuclear explosion. Quantification of the far-field effects from chemical explosive arrays may aid in this discrimination. Preliminary work in this area has been completed by Greenhalgh (1980) (Ref. 10). A complete understanding of the problem relies upon relating the near source models and data to the far-field environment.

The approach to finite explosive arrays reported here will rely on an initial characterization of the single-burst environment. The specific quantification used is from Ref. 11. In that work, the single burst is experimentally quantified with consideration given to source symmetry, propagation path, and scattering. The wave field is divided into a deterministic and stochastic component, with the deterministic component utilized in predictions. Practically, the single-burst quantification is completed in both the time and frequency domain, yielding mean and variance estimates.

In the utilization of the single-burst source quantification, the range of applicability of linear superposition will be tested against experimental data. Once validated, this model will be used to explore finite source effects in the observational data base.

EXPERIMENTAL DESIGN AND IMPLEMENTATION

Each experiment discussed in this report is summarized in Fig. 1. The 5-lb* charges were placed in 1.22-m-deep holes with a diameter of 0.15 m. Charges were placed at the bottom of the hole. The holes were then backfilled with sand.

Force balance accelerometers were used as sensors. The three components (housed in a single case) were oriented in the radial, transverse, and vertical directions with respect to the source. The case was buried in the alluvium so that its top was flush with the free surface. Reference 11 reports the good coherence between 1 and 70 Hz observed when all instruments were placed side-by-side in a huddle test. The accelerometer outputs were passed through a 12-bit analog-to-digital converter in the field and recorded on cassette tape with a sample rate of 200 samples per second. A five-pole antialias filter was placed at 70 Hz.

The test site consisted of dry alluvium and was chosen for its apparent homogeneity. Further discussion of its properties is given in Ref. 11.

As reported in Ref. 11, a number of single-burst experiments were conducted to characterize the source and media with offsets running between 10 and 30 m. The finite source data focused upon the two-explosion case, since these data can be used to constrain the basic characteristics of source interaction. As Fig. 1 illustrates, charge separation was varied between 2 and 10 m at 2-m increments. The proximity of the charges to the free stream (1.22 m) resulted in the formation of craters and significant venting to the free surface at detonation. Crater diameters are given as the solid lines bounding the charge locations in Fig. 1 and were typically near 2 m. ARTS 3 produced a single elongate crater since the lateral charge separation was only 2 m.

*To convert lb to kg, multiply by 4.535 924 E-01.

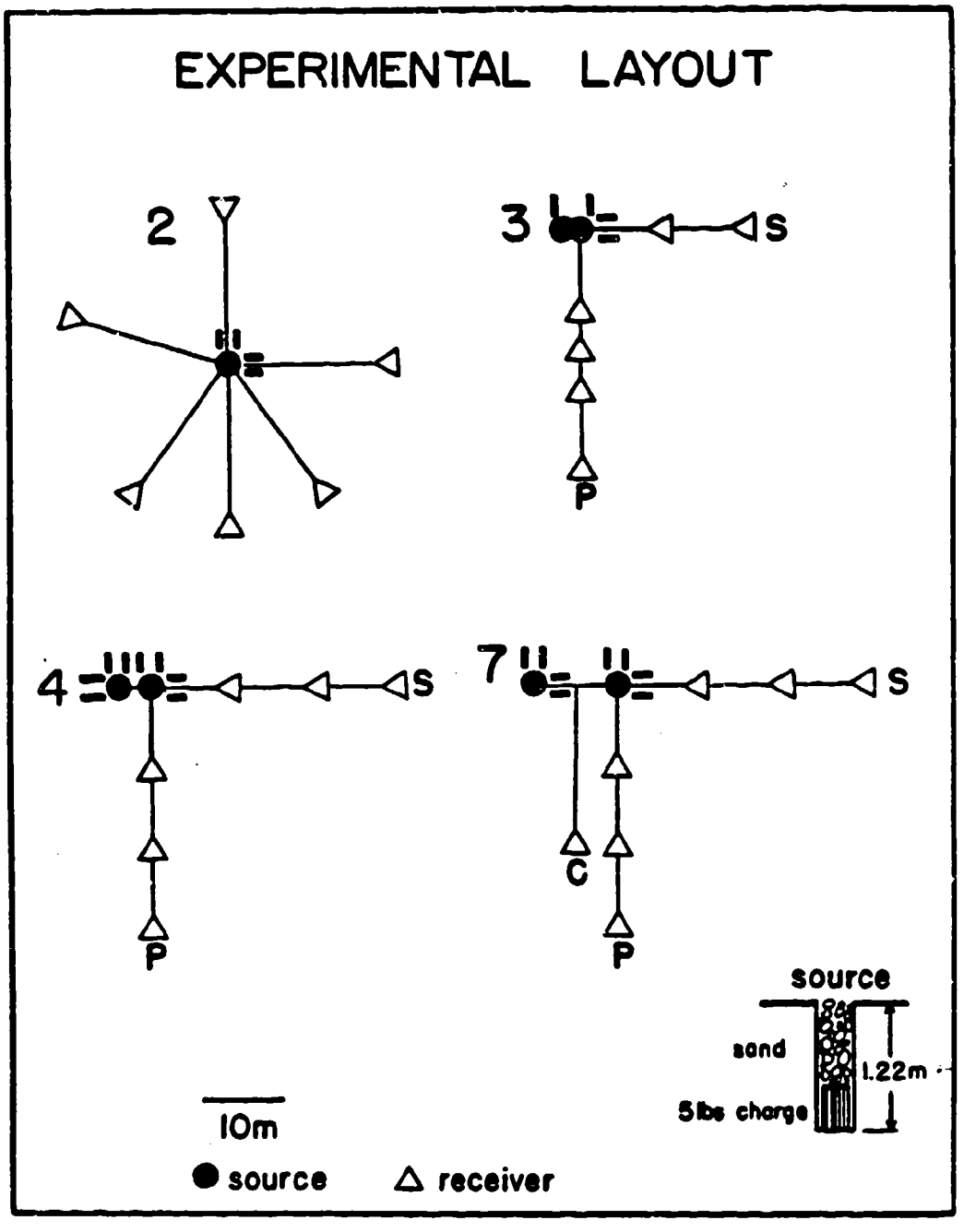

Figure 1. Gauge layout for ARTS 2, 3, 4, 7. (The solid lines indicate crater diameters. Charge placement is illustrated in lower right-hand corner.)

Gauge arrays for the two explosion tests can be separated into two categories. The first set of gauges (primary-P or center-C) were placed at right angles to the plane passing through the charges. These gauge lines intersected either the midpoint between the two charges (C) or one of the charges (P) and were emplaced to check direct superposition. The second set of gauges (secondary-S) were placed in the plane of the charges, and thus the effects of source finiteness were maximized by the travel path and time differences from the two sources (Fig. 1).

SUMMARY OF SINGLE-BURST CHARACTERIZATION

In order to check linear superposition and quantify the effects of finite sources, one must characterize the single explosion source and wave propagation effects at a variety of ranges. ARTS 2 in Fig. 1 is one such test designed to quantify the single source and propagation. A complete discussion of the single source is given in Ref. 11. The time domain records from ARTS 2 are given in Fig. 2. When the records are low-pass filtered at 30 Hz they appear almost identical, while the high-pass-filtered records show significant variations above 40 Hz. A variety of tests were conducted and reported in Ref. 11 to quantify the cause of these high frequency amplitude variations. Strong evidence indicated that scattering within the geological media was responsible for the variation in amplitudes.

This realization led to the calculation of mean and variance estimates for the waveforms from a single explosion at a particular range. Figure 3 is the mean ± 1 standard deviation spectra for the 20-m range from the single burst. Figure 4 is a similar representation, but in the time domain.

The ensemble estimates for the spectra show small variances between 3 and 35 Hz for the 20-m range. Beyond this "coherent frequency," the scatter with azimuth in the data becomes large, as exemplified in the band-pass seismograms of Fig. 2. The 20-m data exhibit 8-dB scatter at 40 Hz.

As reported in Ref. 11, a series of tests were conducted to separate the effects of gauges, gauge placement, source asymmetry, and propagation path on the high frequency data. The variation in the data was attributed to the geological media. Therefore, the deterministic part of the wave field (here defined as the azimuthally symmetric data below 35 Hz) must be the bandwidth of primary focus in the superposition studies.

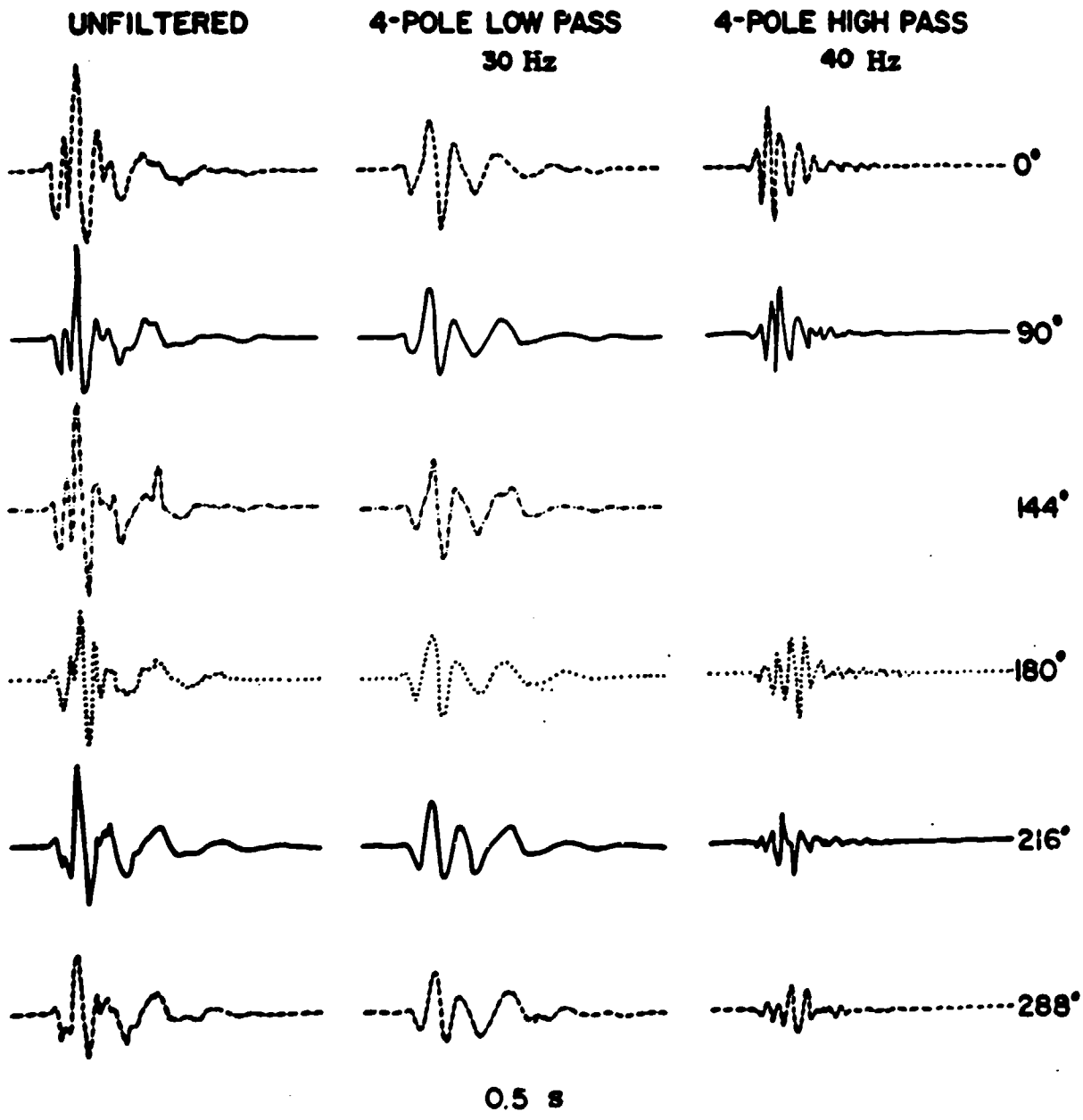

Figure 2. Vertical acceleration records from the ARTS 2 experiment. (All gauges are at 20 m and azimuths range from 0 to 288°. Unfiltered, low-pass filtered (30 Hz), and high-pass filtered (40 Hz) accelerograms are given.)

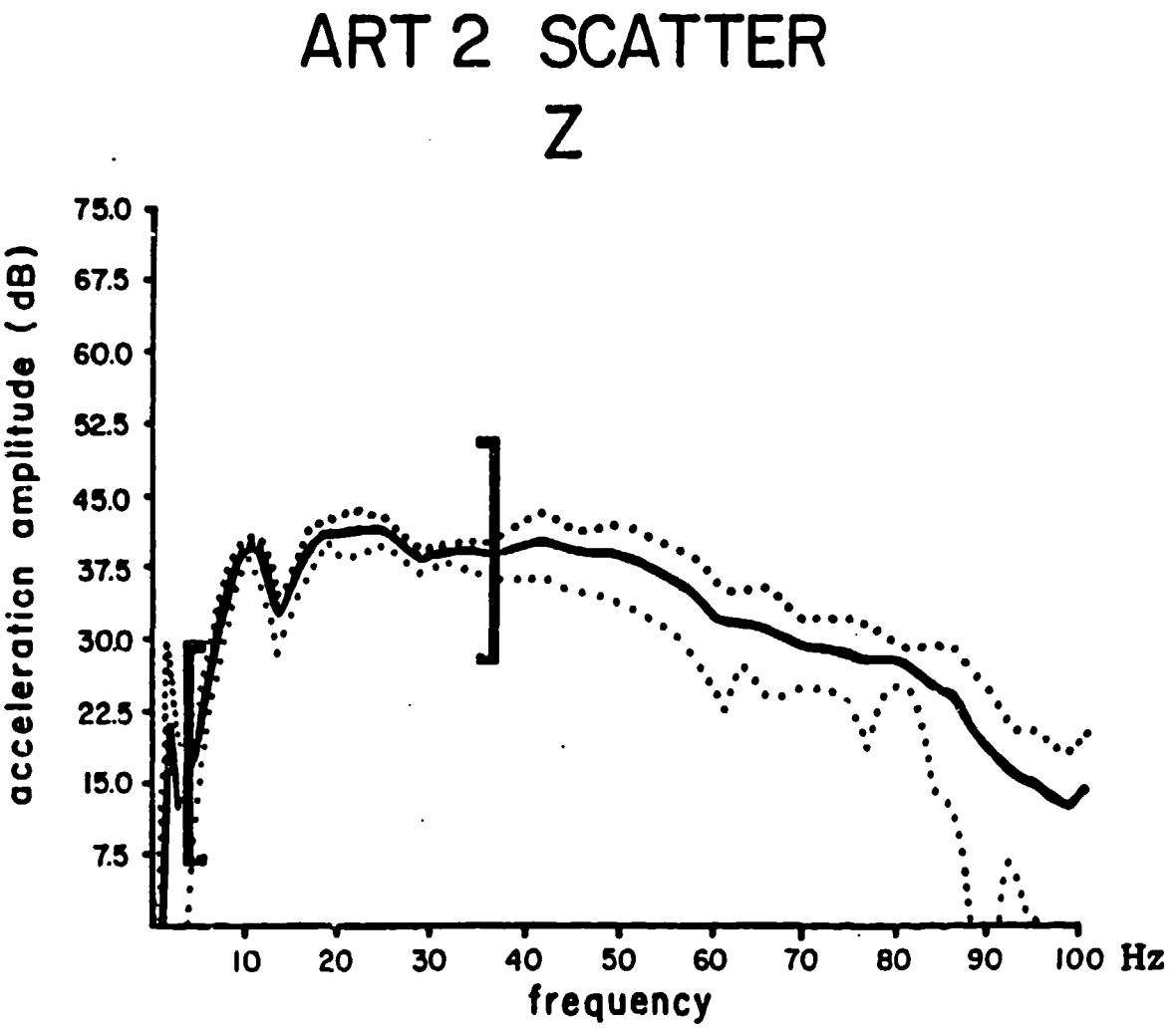

(a) Vertical.

Figure 3. The mean (dark line) and mean ±1 standard deviation (light line) spectral estimate from the 20-m ensemble of ARTS 2.

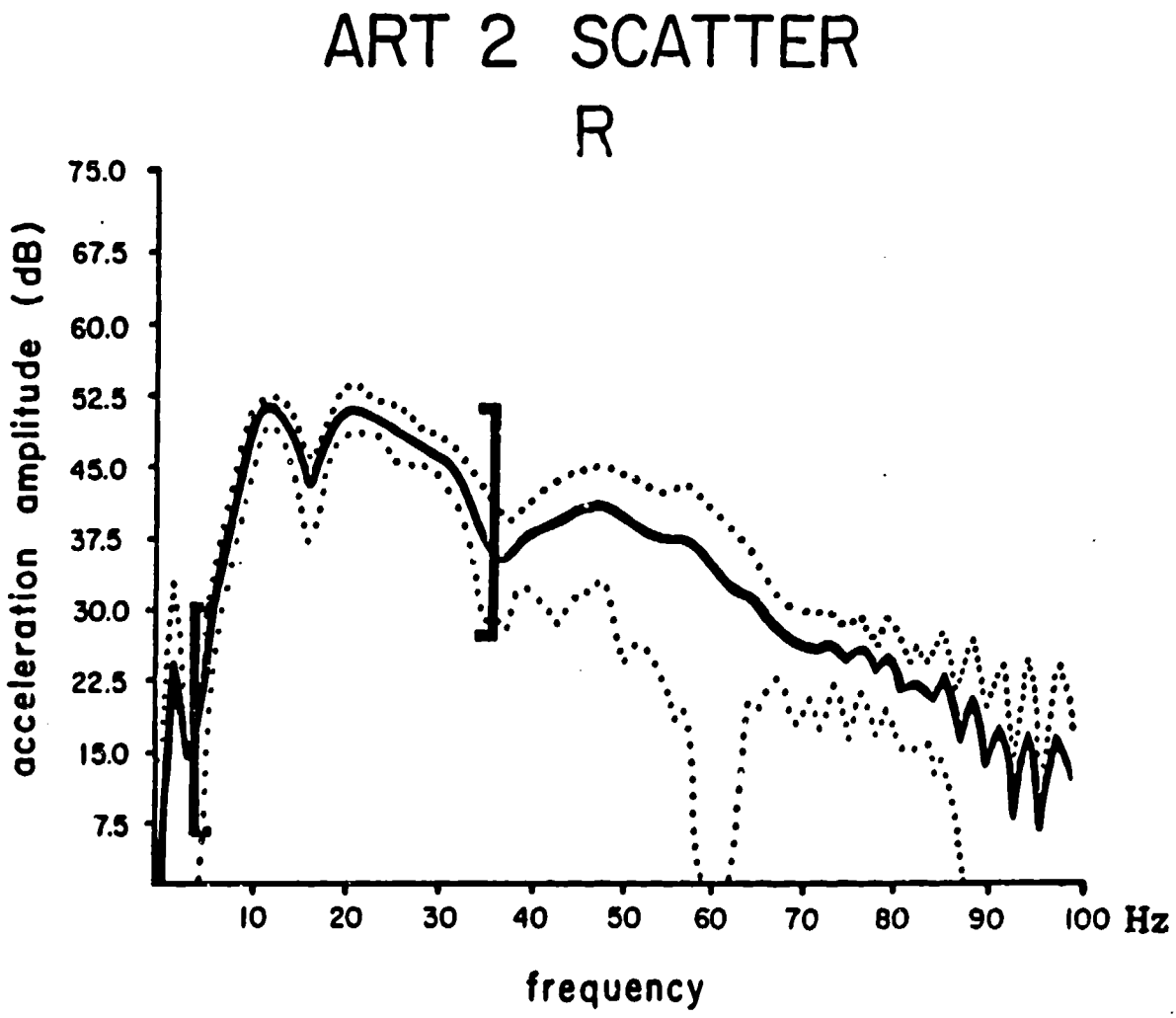

(b) Radial.

Figure 3. Continued.

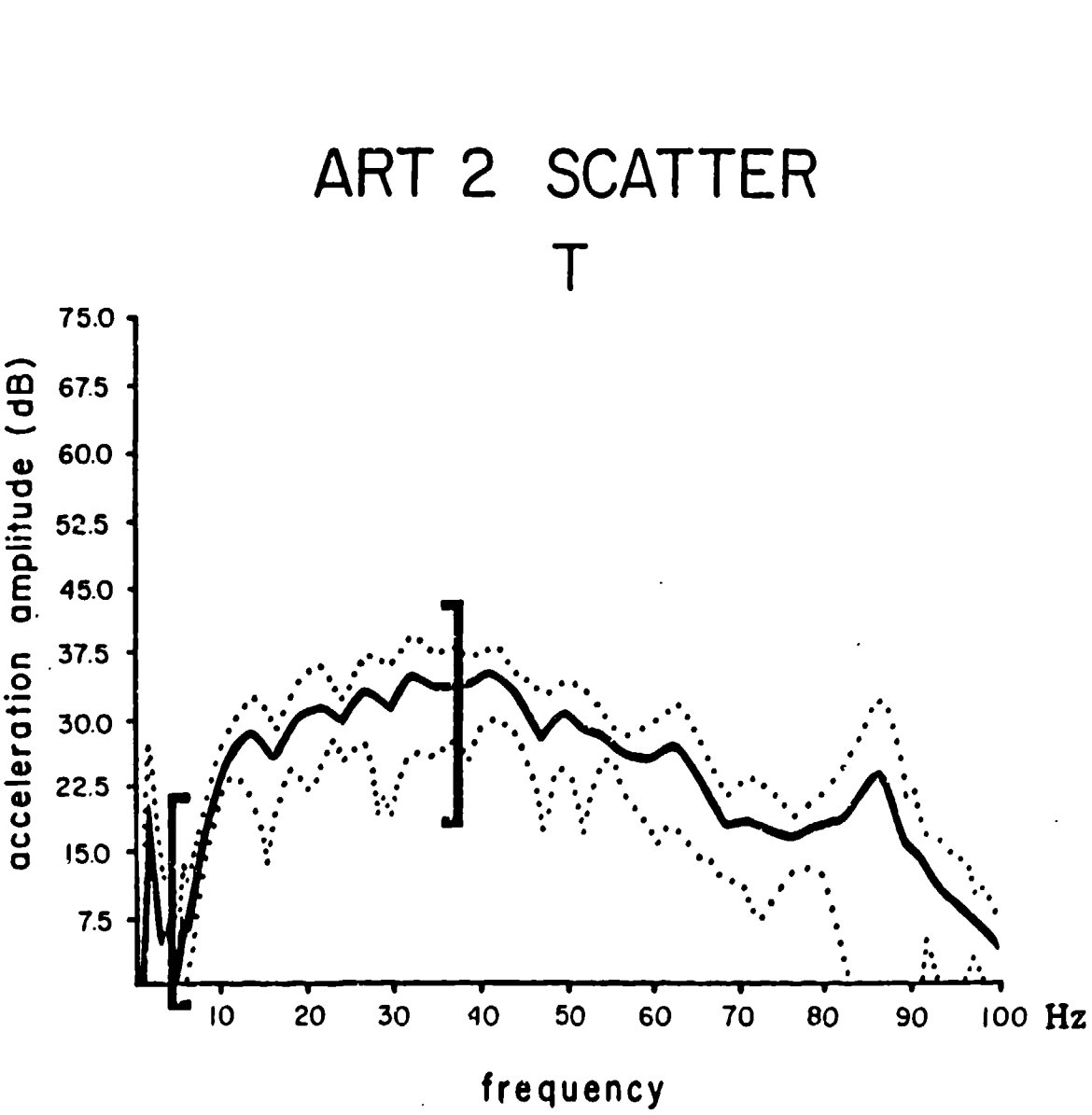

(c) Transverse.

Figure 3. Concluded.

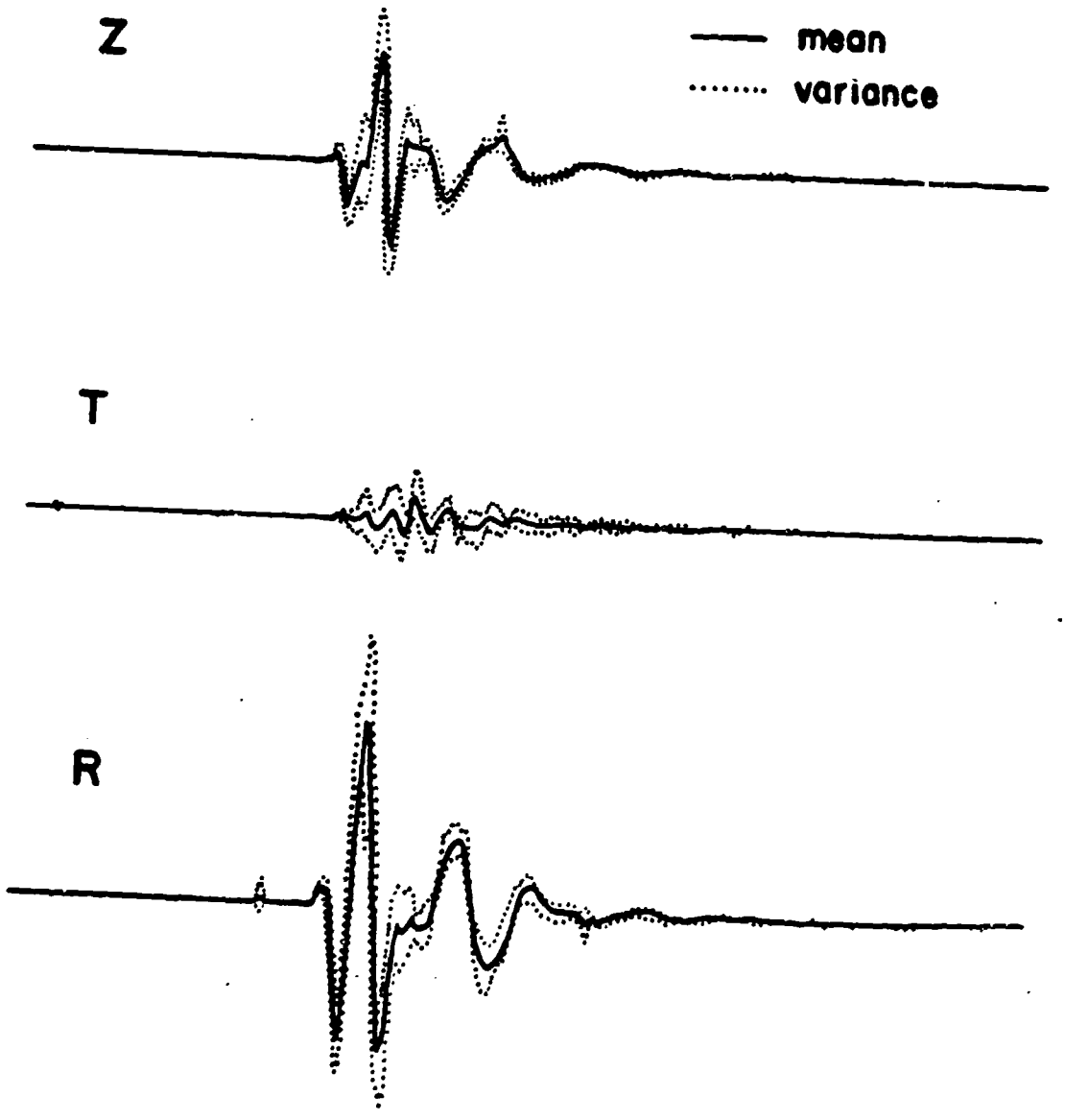

Figure 4. The mean (solid line) and mean ±1 standard deviation (dotted line) time domain estimates from ARTS 2.

SUPERPOSITION

The single-burst ensemble spectral estimates will be used to check the applicability of linear superposition by direct comparison to the multiple-burst data from ARTS 3 and 7 (Fig. 1). The first quantification of these effects will consider the case where each source is equidistant from the charge; thus time delays between the two sources are nonexistent. The primary (P) and center (C) gauge lines are most applicable to this part of the study. Comparisons between the ensemble estimates and the data will be reported only for the 20-m range; however, similar conclusions follow from analysis of data at 10- and 30-m ranges.

Based upon the 3- to 35-Hz coherent bandwidth from the 20-m ensemble estimates, this frequency band is chosen to check superposition. The criterion chosen for valid superposition is that the multiple-burst data fall within ± 1 standard deviation of the ensemble estimate of the multiple-burst environment. Since the stochastic component of the wave field leads to large variances beyond 35 Hz, the criterion is not very robust beyond this frequency.

The 20-m ensemble estimate of the superposed spectra with variances is compared to the P and C gauges for ARTS 3 and 7 in Fig. 5. The vertical observational data compare very well with the superposed spectra between 3-35 Hz. Comparison of the predicted spectra with the observations from ARTS 4, 5, and 6 led to similar conclusions. Each test-bed was displaced approximately 30 m from the previous test, so that between ARTS 2 (used to make single source ensemble estimates) and ARTS 7 the test-bed has been displaced by 150 m. Subtle changes in the geology over these scale lengths may explain the systematic changes in the multiple-burst spectra.

The conclusion to be drawn from this analysis is that, within the variance of the multiple-source estimate, superposition holds for 5-lb charges 20 m from the receiver over the frequency band 3-35 Hz. This includes two charges spaced as close as 2 m where individual craters overlap.

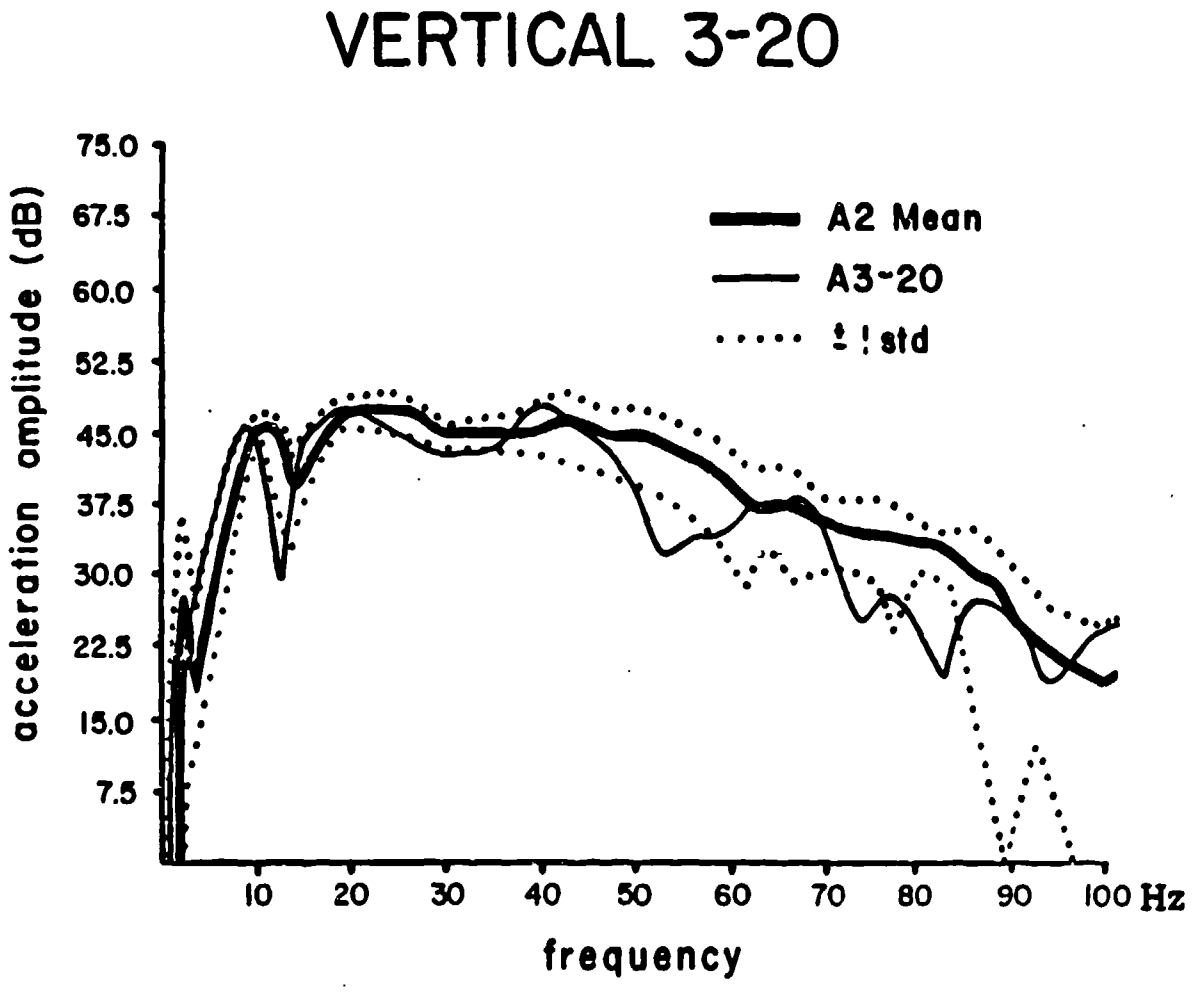

Figure 5a. Predicted and observed superposed acceleration spectra from ARTS 3 with 5-lb charges separated by 2 m.

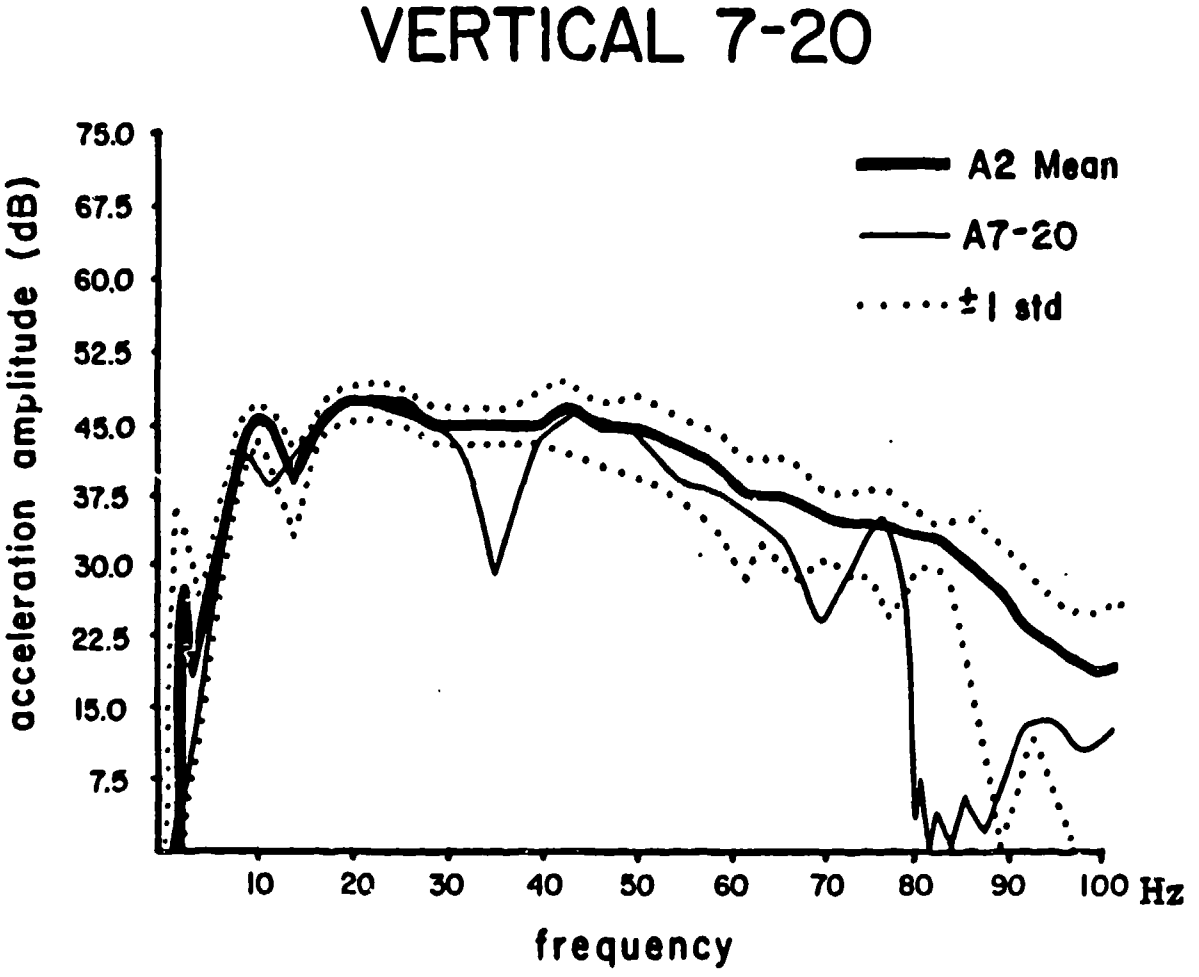

Figure 5b. Predicted and observed superposed acceleration spectra from ARTS 7 with 5-lb charges separated by 10 m.

These results can be compared qualitatively with the reduced displacement potential predicted from the Mueller-Murphy scaling relation (Ref. 12). Figure 6 gives the RDP for a 5- and 10-lb explosion, respectively. The source corner frequency is between 6 and 9 Hz -- remarkably close to what one would estimate from the acceleration spectra (Figs. 3 and 4). The model predicts that below the corner a single charge of 10 lbs will nearly match twice the 5-lb result. Above the corner frequency, the single 10-lb charge will not reach twice the 5-lb result. Thus the critical region for data for testing superposition should fall between 10 and 35 Hz at the [illegible]. The exact location of this range is subject to some error, since the Mueller-Murphy scaling relations were developed for nuclear sources [illegible] er yields. The critical point is that the principal region of interest [illegible] ecking superposition should be beyond the source corner. The [illegible] al results in Fig. 5 support strict superposition well beyond the source corner, with no apparent corner frequency shift.

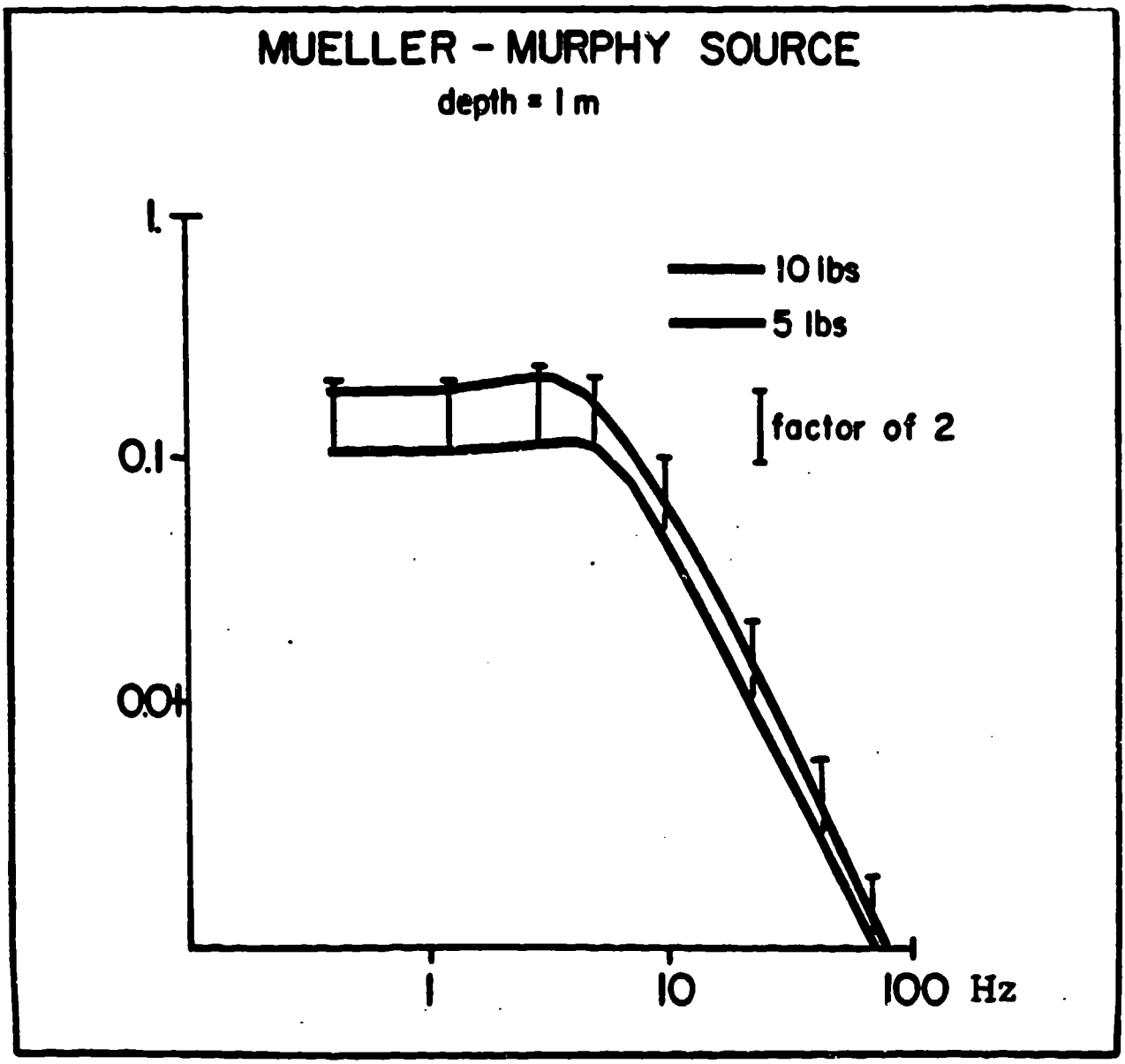

Figure 6. Source displacement spectra predicted by a Mueller-Murphy source model for 5 and 10 lbs of explosive.

RESOLUTION OF SPATIAL FINITENESS

In an attempt to characterize the finite spatial effects of the multiburst environment, synthetics will be compared to data recorded in the plane of the linear array of sources (Fig. 1, secondary (S) lines). The predictions are made utilizing mean seismograms constructed from data such as that generated in the ARTS 2 experiment (Fig. 4).

These mean seismograms are computed by time-aligning the direct P wave from each observation and then computing a mean. The 20-m seismogram from the ARTS 2 experiment, along with its ± 1 standard deviation bound, is given in Fig. 4. The mean radial and vertical accelerograms show little scatter while the transverse component has standard deviations comparable to the mean. This observation is in agreement with the coherent nature of the radial and vertical motions between 4 and 35 Hz and the large scatter for all frequencies of the transverse motion. Since the deterministic component of the wave field is of primary interest in the superposition study, the transverse motion will not be considered.

When two sources are displaced from a receiver at different distances, the following effects occur: (1) a change in arrival time of the radiated energy for one source relative to the other; and (2) a change in the waveform shape, since one contribution has traveled a greater distance than the other. If the receiver to charge separation is relative to the spacing of the two charges, one may neglect the change in wave shape for the two charges. This case is investigated first by superposing the mean seismograms from Fig. 4 with an appropriate delay time for charge separation. The delay time becomes

$$T_D = x_{12}/v$$

where x_{12} is the difference in length of the propagation path for the two charges and v is the velocity of the media. The material at the test site has typical near-surface velocities ranging from 244-366 m/s. These values coupled with charge separation of 2 to 10 m led to a consideration of time delays in the superposition characterization of 5 to 40 ms. The time domain

results of this delay and sum procedure are given in Fig. 7. Qualitative analyses of these results show constructive interference for the direct arriving body waves for very short delay times, 5 ms, with destructive interference leading to complex waveforms for delays between 16 and 30 ms.

Beyond the 30-ms delay, one can begin to observe the individual body waves from the two sources. The surface waves (which arrive at approximately 200 ms into the single-burst observation) show a gradual decay in amplitude over the entire range of delay times with the 40-ms delay yielding a peak amplitude which is four times smaller than that with a 5-ms delay. When the delay times between the two sources are small compared to the single-burst pulse width, constructive interference occurs while complex waveforms with reduced amplitudes are predicted for delay times comparable to the pulse width from a single source wavelet. Figure 8 summarizes amplitude decay changes as a function of delay time for these synthetics.

The frequency domain representation of the superposed waveforms more explicitly exhibits the constructive-destructive interference of the waveforms. The superposed acceleration spectra are compared against the single-burst mean observation in Fig. 9. As quantified in Ref. 13, we observe a modulation of the spectra by

$$\cos(\omega t_D/2)$$

where ω is the angular frequency of interest.

Four qualitative observations of the multiburst spectra are made: (1) the low frequency level of all spectra are identical, reflecting constructive superposition; (2) the point where the spectra diverge from the long period mean occurs at lower frequencies with increasing time delays (arrows in Fig. 9); (3) large spectral holes are observed as predicted with the frequency domain spacing decreasing with increasing time delay between sources; and (4) a return to constructive interference occurs between holes.

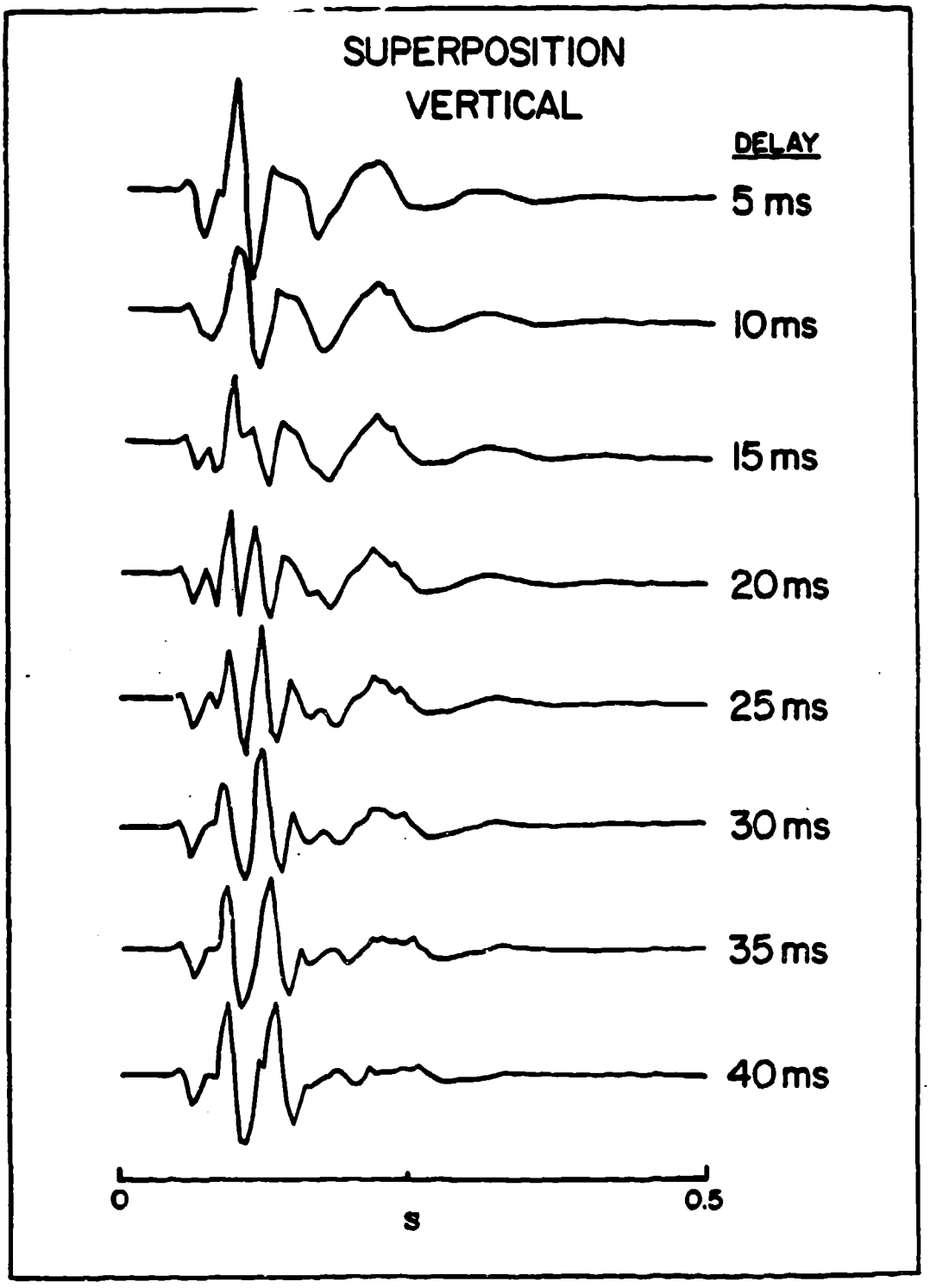

Figure 7. Vertical accelerations from two explosions calculated using the time domain mean seismogram from ARTS 2 and summing with an identical record delayed in time between 5 and 40 ms.

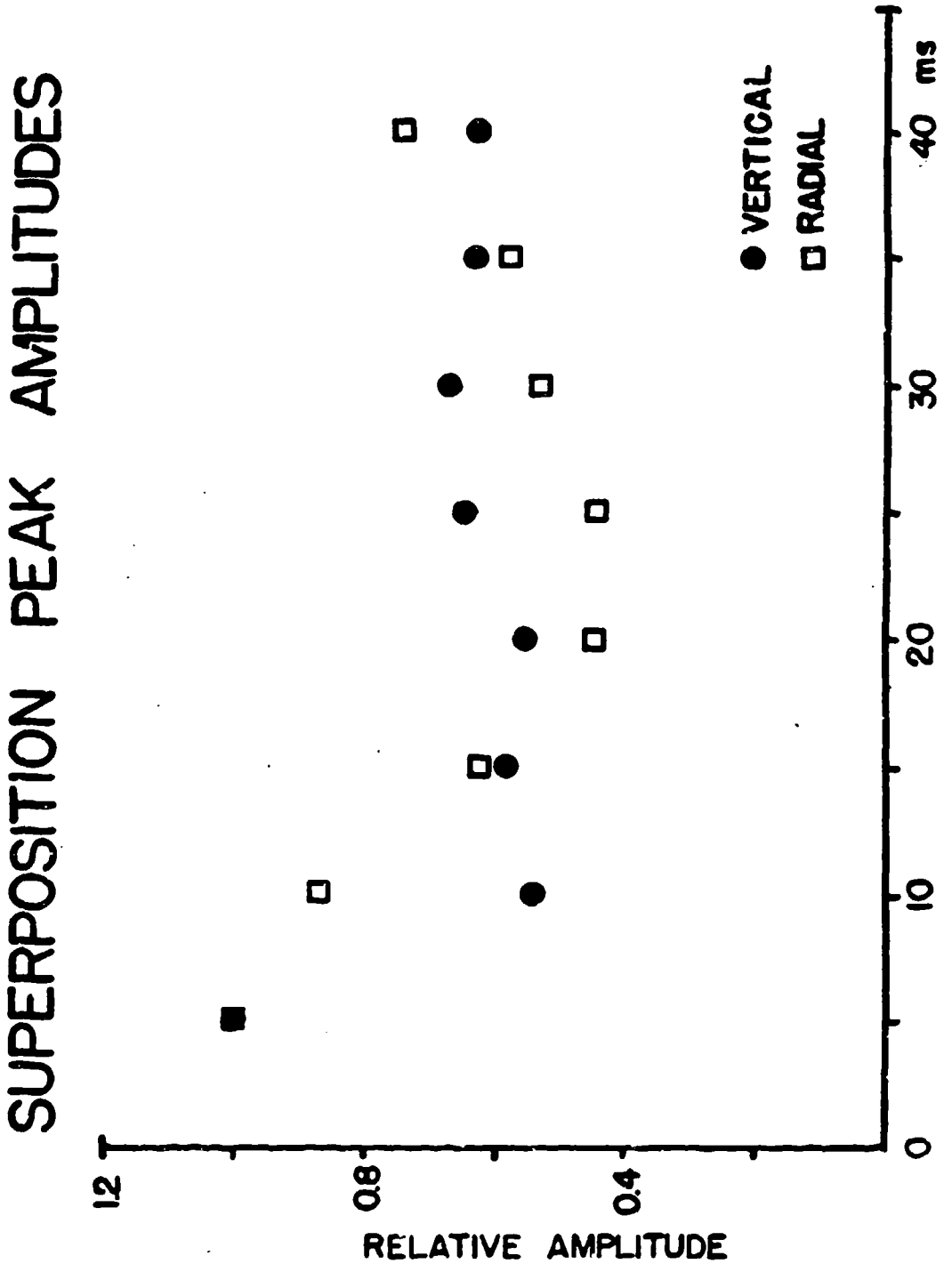

Figure 8. Peak amplitudes of the superposed seismograms from Figure 7 plotted against delay time between the two sources.

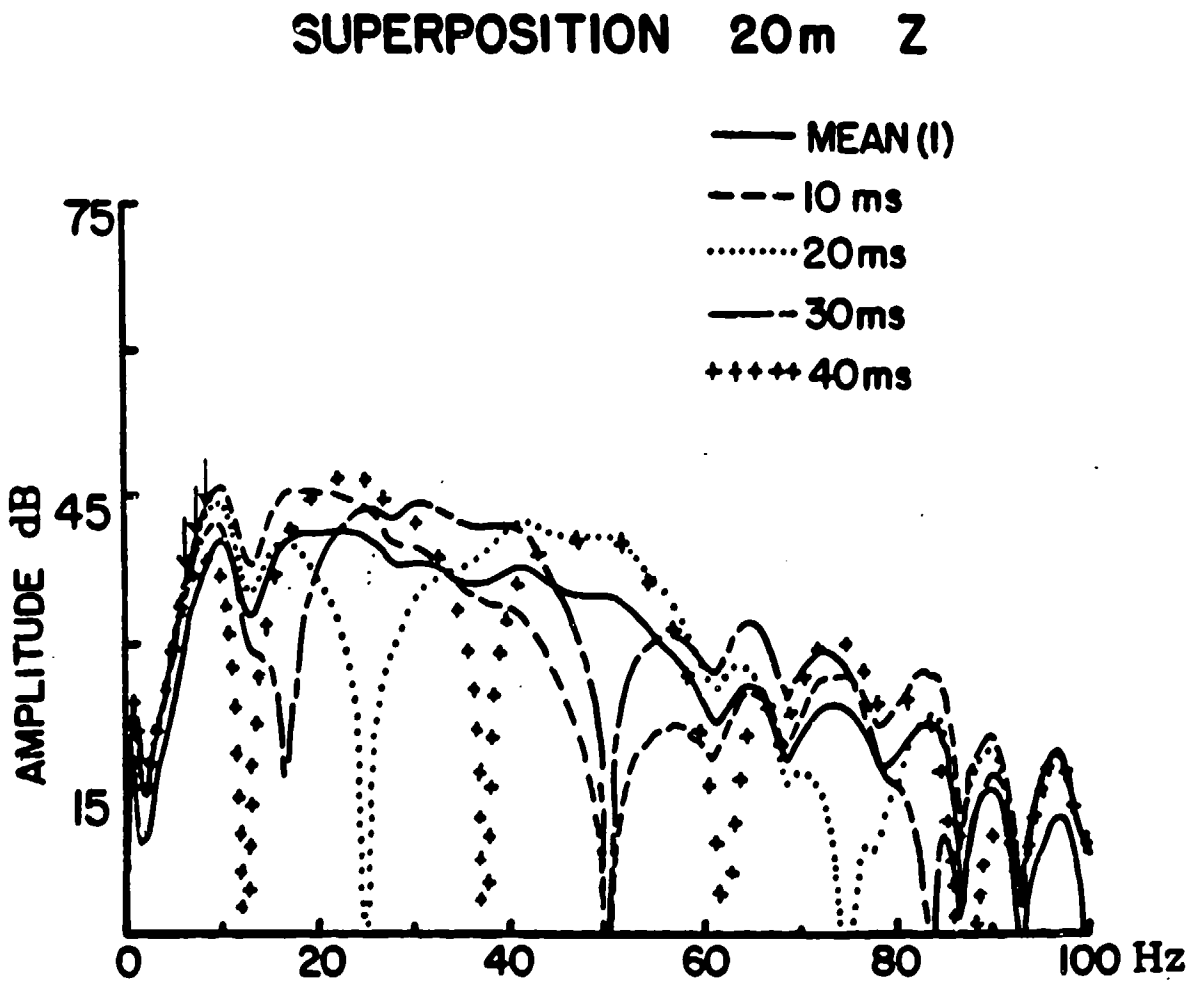

Figure 9. Spectral estimates of the superposed accelerations from Figure 7.

These results assume no change in the Green's functions or propagation path effects as the charge separation increases. The vaiidity of this assumption can be checked against the multiburst observational data (Fig. 10). The secondary gauge lines in the plane of the charge array yield the necessary data.

The primary, secondary and A2MEAN (predicted linear superposition acceleration spectra) for event 4 (4-m separation) at 20-m range and event 7 (10-m separation) at 20-m range are given in Figs. 10a and 10b. As already noted in the superposition discussion, the primary gauge and A2MEAN prediction overlay one another between 2 and 35 Hz. The effect of charge separation is maximized for the secondary gauge, where for event 4 the two charges are 20 and 24 m from the gauge, and for event 7 the two charges are 20 and 30 m from the gauge. The spectral scalloping already noted in the synthetics is well defined for event 4 but reduced in scope for event 7. The overall amplitudes for the secondary gauges are reduced throughout the bandwidth for both experiments.

Figure 11 gives the secondary gauge data for event 4, along with the prediction utilizing the mean 20-m data delayed by 15 ms. The prediction closely replicates the observational data, including the large spectral hole at 32 Hz. The 15-ms delay time replicates a propagation velocity of 266 m/s between the two closely spaced charges. This velocity is near the surface wave velocity, suggesting surface wave contribution is dominant. Thus for charges spaced as closely as 4 m and observed at 20 and 24 m, respectively, the waveform can be replicated by superposing two 20-m single-burst waveforms. We conclude that over these close ranges the Green's functions change slowly and that the primary effect on the superposed waveforms is a time delay.

For event 7, the 20-m secondary observations are 20 and 30 m from the two charges. The change in propagation path effects for the 20- and 30-m ranges were dramatic enough so that successful prediction required the mean seismograms from single bursts at 20 and 30 m respectively. The 30-m mean seismogram was calculated in the same way as that for 20 m given in Fig. 4.

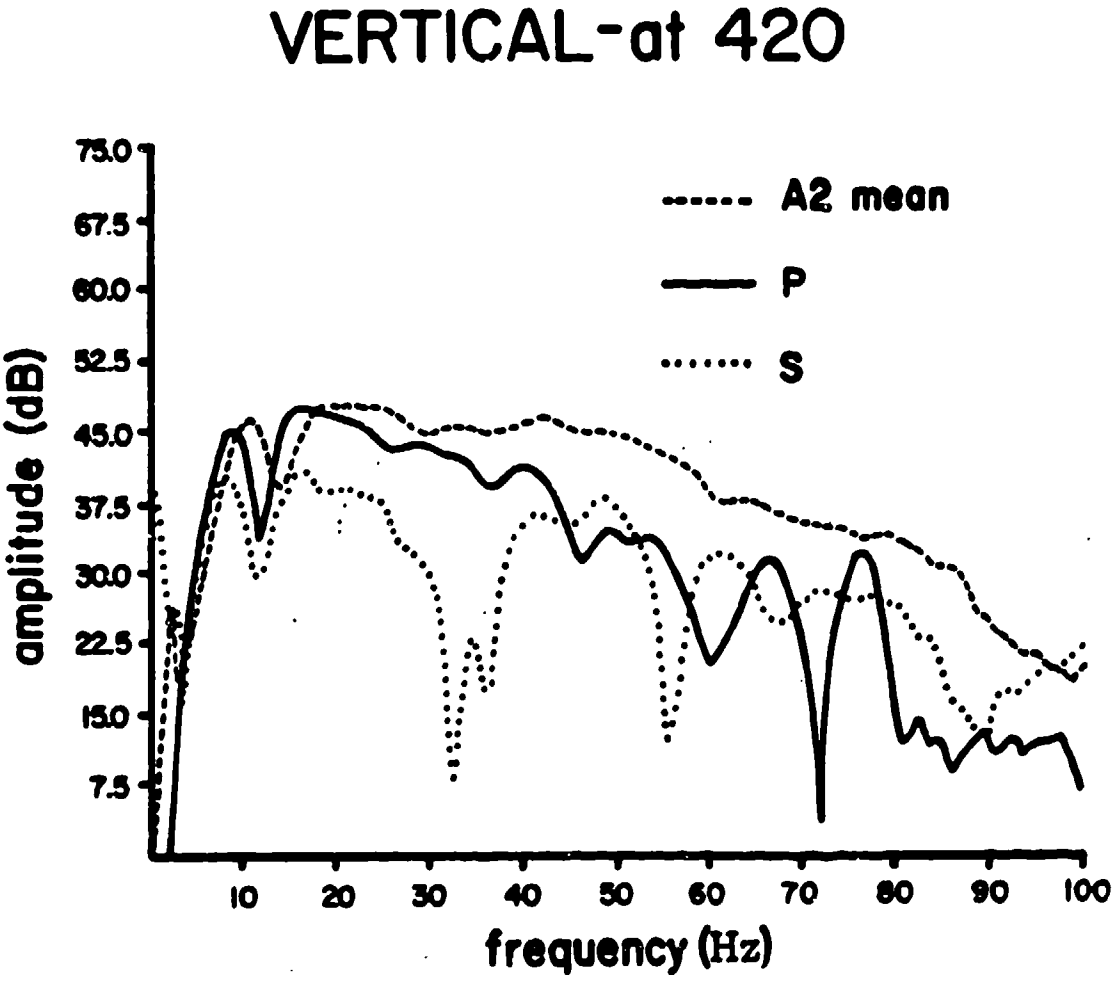

Figure 10a. The primary (P), secondary (S) observations and predicted superposition (A2 mean) for ARTS 4.

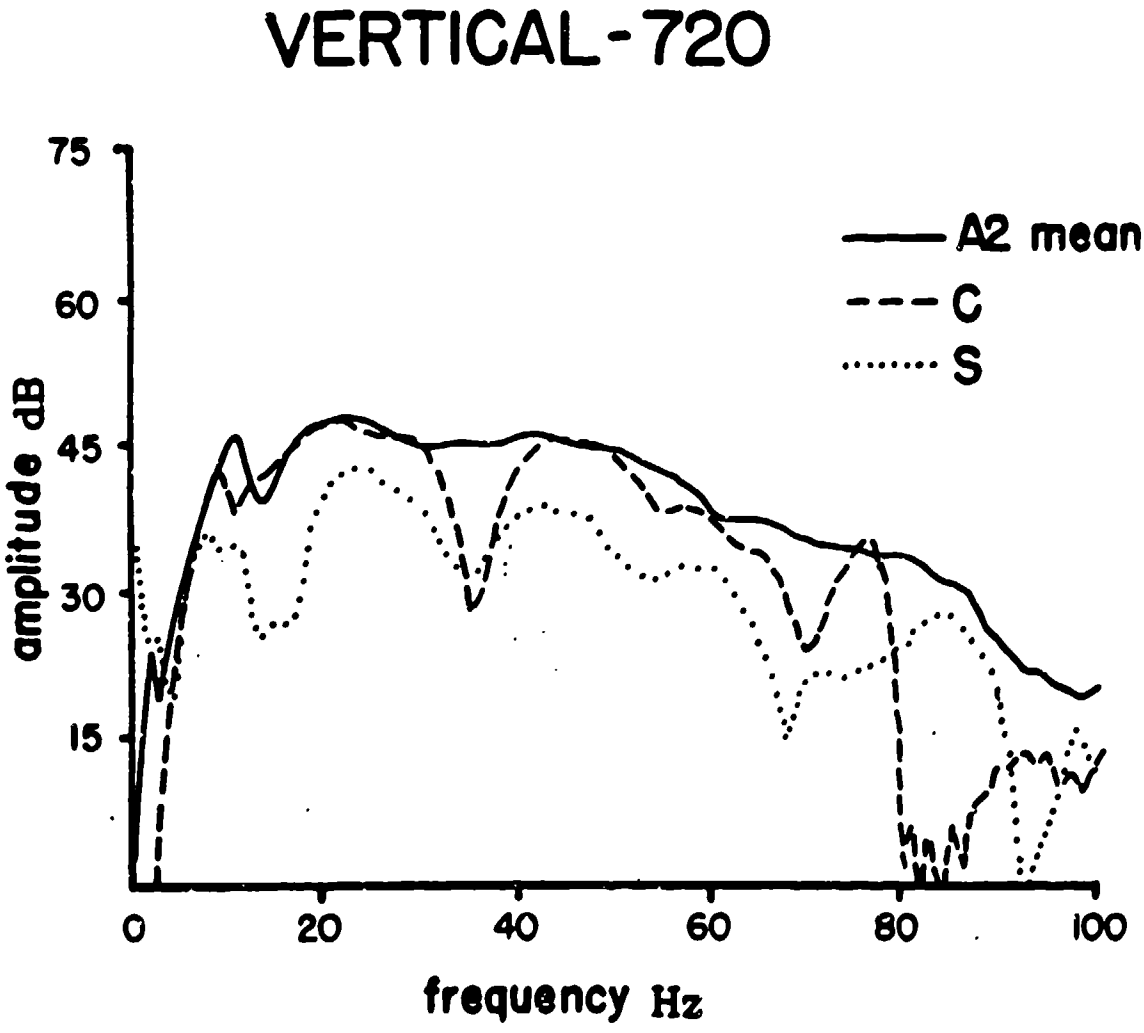

Figure 10b. The primary (P), secondary (S) observations and predicted superposition (A2 mean) for ARTS 7.

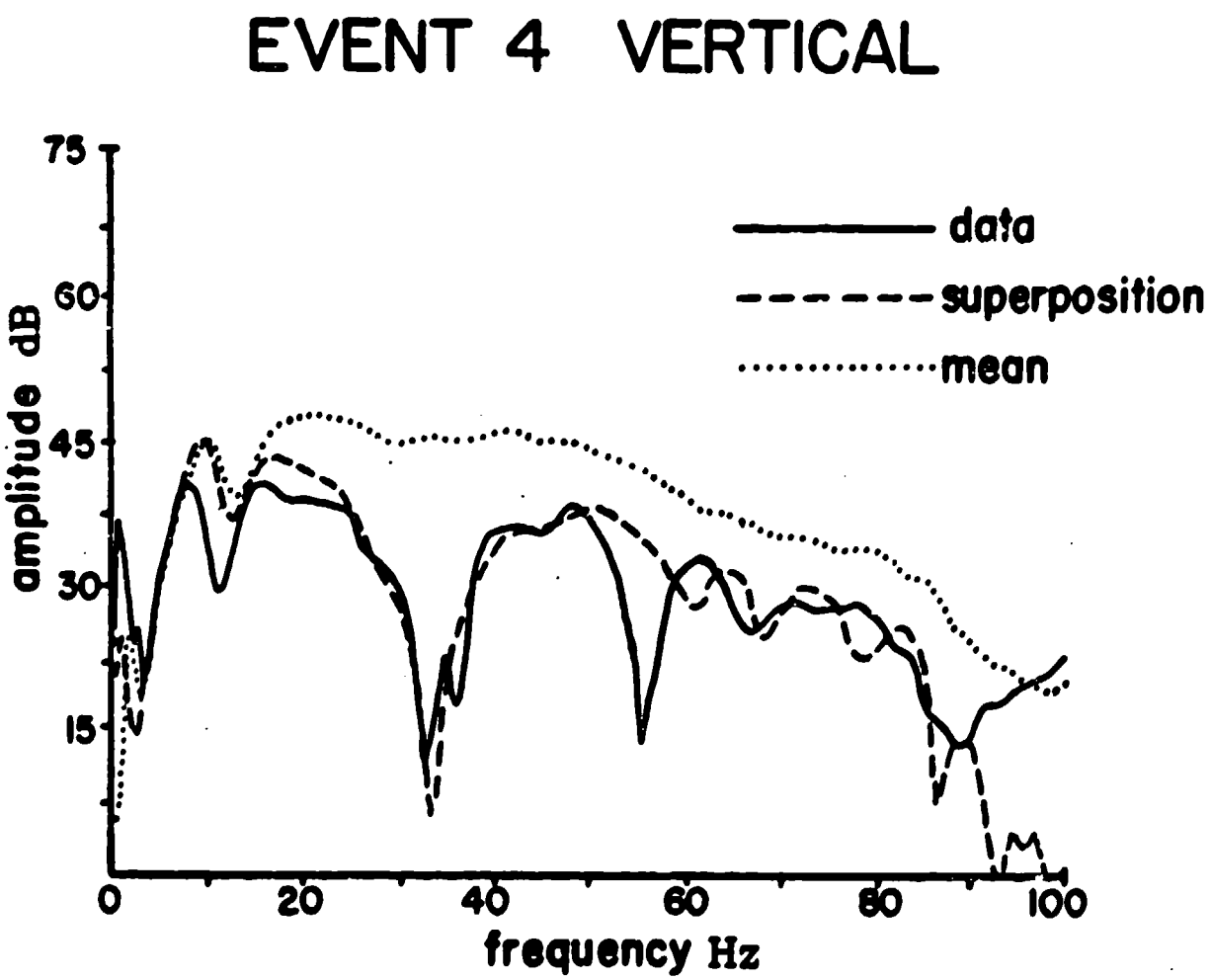

Figure 11. The predicted superposition spectra for two charges at 20 and 24 m (ARTS 4 - secondary) compared to the data and superposition with no delay time (mean).

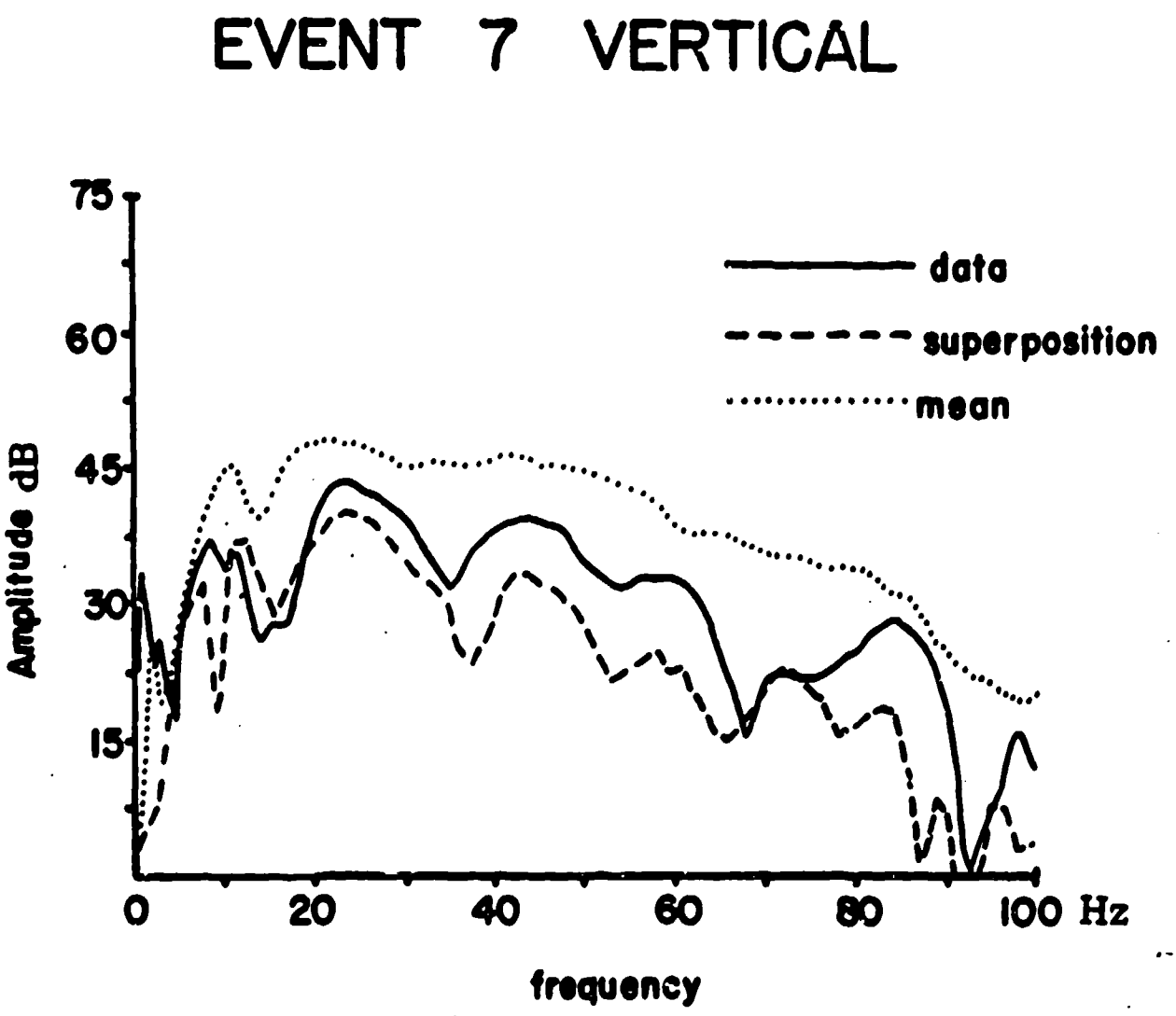

Figure 12. The predicted superposition spectra for two charges at 20 and 30 m (ARTS 7 - secondary) compared to data and superposition with no delay time or propagation differences (mean).

Figure 12 displays the prediction and observations for event 7. One initially notes the closer spaced spectral nulls representative of the 25-ms delay time. Due to the change in propagation path between the two sources, the spectral nulls are much smoother and not as deep as those observed when two identical sources are superposed (Fig. 10).

There are three propagation effects which lead to the necessity of including mean seismograms from each of the two sources in ARTS 7: (1) a significant change in $t_s - t_p$ time; (2) strong geometrical spreading effects; and (3) attenuation. A simple analysis of these effects can explain the success of the ARTS 4 superposition using the 20-m mean seismograms and the failure of ARTS 7 utilizing the 20-m range waveform. Taking the near surface velocities as $\alpha = 366$ m/s, $\beta = 244$ m/s (Ref. 14), the ARTS 4 S-P time difference for the two shots is 0.005 s and ARTS 7 time difference is 0.014 s. The 0.005-s change is one sample interval and results in phase shifts ranging from 31° at 17 Hz to 63° at 35 Hz. For ARTS 7 the phase shift is 86° at 17 Hz to 176° at 35 Hz. The phase shifts for ARTS 7 are dramatic enough to jeopardize the single waveform superposition procedure. At higher frequencies the ARTS 4 results should also deteriorate.

Geometrical spreading will lead to amplitude differences from the two sources which are not accounted for in the single seismogram superposition. Experimental geometrical decay rates for this test site give $r^{-1.6}$ for the body wave and $r^{-0.5}$ for the surface waves (Ref. 15). For ARTS 4, with charges at 20 and 24 m, the ratio of body wave amplitudes is predicted to be 0.75 while the ratio of surface wave amplitudes is 0.93. Similar calculations for ARTS 7 give the body wave ratio as 0.54 and the surface wave ratio as 0.82. These calculations indicate that, at least for the body waves, the single range superposition procedure for ARTS 7 is inadequate.

Finally, the effect of attenuation must be quantified. The range of Q values for the dry alluvium environment can be bounded between 10 and 40 (Ref. 16). Taking the simple exponential Q model $e^{-\pi ft/Q}$, where we use f as the frequency and t as the shear arrival time, Table 1 was developed to quantify these results for the 3-35 Hz band. The 24-m to 20-m ratios show only

TABLE 1. Values of $e^{-\pi ft/Q}$

20-m Range

f	Q 10	20	40
35	0.41	0.64	0.80
17.5	0.64	0.80	0.89
8.75	0.80	0.89	0.95

24-m Range

f	Q 10	20	40
35	0.34	0.50	0.76
17.5	0.58	0.76	0.87
8.75	0.76	0.87	0.93

30-m Range

f	Q 10	20	40
35	0.26	0.51	0.71
17.5	0.51	0.71	0.84
8.75	0.71	0.84	0.92

Ratio 24 m/20 m

f	Q 10	20	40
35	0.83	0.91	0.95
17.5	0.91	0.95	0.98
8.75	0.95	0.98	0.98

Ratio 30 m/20 m

f	Q 10	20	40
35	0.63	0.78	0.89
17.5	0.79	0.89	0.94
8.75	0.89	0.94	0.97

moderate Q effects even at the highest frequencies and smallest Qs. The 30-m to 20-m ratios give a value of 0.63 for Q = 10 and f = 35 Hz. Although the Q effects are less dramatic than the phase shifts and geometrical spreading terms, they may become significant for ARTS 7 but are negligible for ARTS 4.

CONCLUSION

The series of small-scale explosive experi[illegible]bility of linear superposition in the near-field. Th[illegible]ne must separate stochastic and deterministic propegat[illegible] single-burst wavefield prior to hypothesis test[illegible]e has been completed (Ref. 11), then superposition is[illegible]st wavefield falls within ±1 standard deviation of [illegible]within the coherent bandwidth (3-35 Hz)]. Thus superp[illegible] two 5-lb charges spaced as closely as 2 m. Compari[illegible]phy source function for 5 and 10 lbs shows that superposition must be checked above the source corner frequency.

Finite spatial source effects are experimentally quantified by recording data in the plane of the two charges. These finite effects in the near-field include: (1) rise in long period spectral values that match direct superposition; (2) lowering of corner frequency with increased source separation; and (3) spectral scalloping at high frequencies. Comparison of superposed ensemble spectra (time delayed) shows that, when travel time differences between the two sources are the primary effects in the observed wavefield, then the observed data which include large interference holes in the spectra are replicated. As propagation path differences between the two charges result in waveform changes, the superposition procedure can be applied using separate ensemble wavefield estimates for each range. The resulting predicted waveforms again match observations which include direct superposition at long periods and spectral levels which are reduced above the corner frequencies. Interference holes which were so prevalent when only source time delays were present (ARTS 4) are not nearly so well defined when wave shape changes due to propagation are present in the superposition (ARTS 7). ARTS 4 included sources 20 and 24 m from the receiver, which could be replicated using only a time delay between the two sources. ARTS 7, with sources at 20 and 30 m from the receiver, required the inclusion of waveform changes in order to replicate the observational data. These propagation effects were quantified with the change in S-P time between the two charges leading to large phase shifts for ARTS 7. Differences in geometrical spreading and Q for the two charges in ARTS 7 were important, although not as strong.

Utilizing the principles of superposition as applied to the deterministic portion of the wavefield, a procedure has been developed which can be used to predict waveforms from large arrays of explosives. This procedure assumes that the single burst environment has been characterized and may require the environment to be quantified at a number of ranges when arrival time differences, geometrical spreading differences, and attenuation differences are important. Arrival time and attenuation differences increase with frequency.

REFERENCES

1. Winzer, S.R., The Firing Times of ms-Delay Blasting Caps and Their Effect on Blasting Performance, Report to the National Science Foundation, Contract DAR-77-05171, Martin Marietta Laboratories, Baltimore, Maryland, 1978.

2. Bergnam, O.R., Wu, F.C. and Edl, J.W., "Model Rock Blasting Measures Effects of Delays and Hole Pattern on Rock Fragmentation," Engineering Mining Journal, Vol. 175, No. 6, pp. 124-127, 1974.

3. Hagan, T.N. and Just, G.D., "Rock Breakage by Explosives: Theory, Practice, and Optimization," Proc. Third Int. Soc. Rock Mech., Vol. 2, pp. 1349-1358, 1974.

4. Winzer, S.R., and Ritter, A.P., "The Role of Stress Waves and Discontinuities in Rock Fragmentation: A Study of Fragmentation in Large Limestone Blocks," Proc. 21st U.S. Symposium on Rock Mechanics, University of Missouri, Rolla, Missouri, pp. 362-370, 1980.

5. Winzer, S.R., Anderson, D.A., and Ritter, A.P., "Application of Fragmentation Research to Blast Design: Relationships Between Blast Design for Optimum Fragmentation and Frequency of Resultant Ground Vibration," Proc. 22nd U.S. Symposium on Rock Mechanics, MIT, Cambridge, Massachusetts, pp. 237-241, 1981.

6. Anderson, D.A., Winzer, S.R., and Ritter, A.P., "Blast Design for Optimizing Fragmentation While Controlling Frequency of Ground Vibration," Proceedings of the 8th Annual Conference on Explosive and Blasting Techniques, New Orleans, Louisiana, pp. 69-89, 1982.

7. Higgins, C.J., Johnson, R.L., and Triandafilidis, G.E., "The Simulation of Earthquake-like Ground Motions with High Explosives," Report CE-45 (78) NSF-507-1, Department of Civil Engineering, University of New Mexico, Albuquerque, New Mexico, 1978.

8. Bleisweis, B., et al., "Simulation of Strong Motion Earthquake Effects on Structures Using Explosive Blasts," Nuclear Engineering and Design, Vol. 25, pp. 126-149, 1973.

9. Cooper, H.F., On the Simulation of Ground Motions Produced by Nuclear Explosions, AFWL-WLC-TN-70-001, Air Force Weapons Laboratory, Kirtland AFB, New Mexico, 1970.

10. Greenhalgh, S.A., "Effect of Delay Shooting on the Nature of P-wave Seismograms," Bull. Seism. Soc. Am., 70, pp. 2037-2050, 1980.

11. Reinke, R.E., and Stump, B.W., Stochastic Geologic Effects on Near-Field Ground Motion in Alluvium, AFWL-TR-86-133, Nov 1987.

REFERENCES (concluded)

12. Mueller, R.A., and Murphy, J.R., "Seismic Characteristics of Underground Nuclear Detonations: Part I, Seismic Scaling Law of Underground Nuclear Detonations," Bull. Seism. Soc. Am., 61, pp. 1675-1692, 1975.

13. Pilant, W.L., and Knopoff, L., "Observations of Multiple Seismic Events," Bull. Seism. Soc. Am., 54, pp. 19-39, 1964.

14. Stump, B.W., and Reinke, R.E., Spall-like Waveforms Observed in High-Explosive Testing in Alluvium, AFWL-TR-82-15, Air Force Weapons Laboratory, Kirtland AFB, New Mexico, Sep 1982.

15. Stump, B.W., "Source Characterization of Bermed Surface Bursts," Bull. Seism. Soc. Am., 73, pp. 979-1003, 1983.

16. Flynne, E.C., "Effects of Source Depth on Near Source Seismograms," M.S. Thesis, Southern Methodist University, Dallas, Texas, 1986.